SLAC – PUB – 5719
October 1991
T/E

FUTURE FACILITIES FOR LIGHT QUARK SPECTROSCOPY: A PERSPECTIVE BASED ON THE LASS EXPERIENCE*

BLAIR N. RATCLIFF

Stanford Linear Accelerator Center, Stanford University, CA 94309, USA

ABSTRACT

Some desirable design features of a future facility for the study of light meson spectroscopy in hadroproduction are described and compared with what has been achieved by the LASS spectrometer. A few aspects of next-generation experiments using such a facility are also discussed, including final state sample sizes and performance requirements. The need for complementary production modes and decay channels, and the importance of a broad programmatic approach to the physics are stressed.

MOTIVATION

A number of talks in this session have already discussed the possibilities for providing medium energy, high flux beams suitable for future hadroproduction experiments at a number of accelerators.[1] In this talk, I will indulge in a few general remarks about light quark spectroscopy, and the design of an experimental facility to fit in such a beam line. I will illustrate these remarks with results from the programmatic studies of strange and strangeonium mesons in K^-p production with the LASS spectrometer at SLAC.[2–17]

It must be realized at the outset that any new experimental attempt to address the broad questions of light hadron spectroscopy will be a major effort requiring a very high quality spectrometer and extensive analysis of massive data samples. After all, the physics has been studied for well over 20 years in many different production environments, and, in many cases, with very large data samples. In these circumstances, it seems fair to ask whether the pursuit of this physics justifies the effort.

A candidate theory of the strong interactions (QCD) has been under development since the early 1970's, but it is still not possible to calculate the spectrum reliably. In the future, if high quality calculations of the QCD spectrum were to become available (perhaps from the lattice), detailed quantitative comparisons with the experimental spectrum would be the ideal test of the theory. However, at the moment, our theoretical understanding of $q\bar{q}$ hadronic structure remains based largely on "new" versions of old-fashioned constituent quark models, very similar to those that have been in existence for about 25 years.[18] In this approximation, comparisons are made more reliably in the heavy spectroscopies, and so it might be argued that experimental effort is better spent on the heavy particles. Moreover, in a more fundamental sense, it can be argued that studies at high energies, away from the bound state regime altogether, are likely to be more profitable.

* Work supported by the Department of Energy under contract No. DE-AC03-76SF00515.

Invited talk at the International Conference on Hadron Spectroscopy, College Park, Maryland, August 12–16, 1991

However, the scale of the effort required to make major experimental progress in the light meson sector, while not small, is quite modest compared to most studies at higher energies; and even though many detailed properties of the light quark spectra have not been understood in 20 years of study, we have learned how to do much better experiments. Thus, it can be argued that the experiments should be done, even though we can not now calculate the details precisely. There are a number of reasons why such data could be helpful at this time. One of the clearest predictions of QCD is that exotic hadrons should exist in addition to those predicted by the naive constituent quark models. The presence or absence of these states is a crucial qualitative test of the theory. None of the predicted exotics have been unambiguously identified to date.

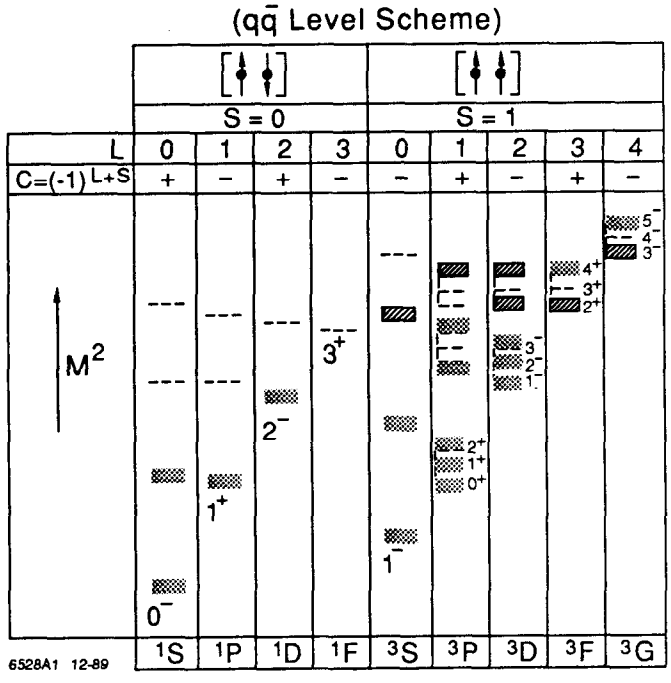

Fig. 1 Level diagram (Grotrian plot) for the strange meson states observed in LASS. The dashed lines indicate the lowest lying states expected in the quark model. The mass levels are illustrative only. The states indicated by cross-hatching are clearly observed, and have generally been confirmed; in a few cases there are possible classification ambiguities. The states indicated by diagonal lines are more speculative and require confirmation.

Since most of these states can hide amongst the normal $q\bar{q}$ states, it is very important to provide an accurate template of $q\bar{q}$ states against which to compare exotic candidates.

The $q\bar{q}$ spectra are known to agree well with the simple models; and, in particular, the qualitative features seem clear. Figure 1 shows the known spectrum of strange states as observed in LASS and its predecessor experiments at SLAC.[2-17,19] The observed states are those expected in the model; the orbital excitations lie on approximately linear trajectories; and the $L \cdot S$ triplet splittings seem to be small. The strange mesons provide an excellent laboratory to study a pure $q\bar{q}$ system since there is no isoscalar-isovector mixing and no confusion with pure glueballs, and indeed, this spectrum is the best understood of the mesonic spectra. However, there are only a few states whose parameters are very well measured (to $\sim$ 10 MeV/c^2 or better). More data would help to confirm the features and pin down the parameters, and in the case of other sectors (e.g. $s\bar{s}$) the data need to be expanded by about two orders of magnitude just to match the experimental situation in the strange sector.

In the following, I will discuss some of the features of a facility which could perform such experiments. This will be preceded by a review of LASS to illustrate why some of these features are desirable.

THE LASS EXPERIMENT

The LASS facility, shown in Fig. 2, is a general purpose spectrometer designed primarily for meson spectroscopy.[2] It has 4π geometrical acceptance with excellent angular and momentum resolution, full azimuthal symmetry, excellent particle identification, and high rate data acquisition capability. LASS contains two large magnets filled with tracking detectors. The first magnet is a superconducting solenoid with a 22.4 kG field parallel to the beam direction. This is followed by a 30 kG-m dipole magnet with a vertical field. The solenoid is effective in measuring the interaction products which have large production angles and relatively low momenta. High energy secondaries, which tend to stay close to the beam line, are not well measured in the solenoid, but pass through the dipole for measurement there.

Particle identification is provided by a Cherenkov counter (C_1) and a time-of-flight hodoscope (TOF) which fill the exit aperture of the solenoid, and by a Cherenkov counter (C_2) at the exit of the dipole spectrometer. In addition, the dE/dx ionization energy loss in the cylindrical proportional chambers which surround the target is measured to separate wide angle protons from π's in the $1/\beta^2$ region below 600 MeV/c.

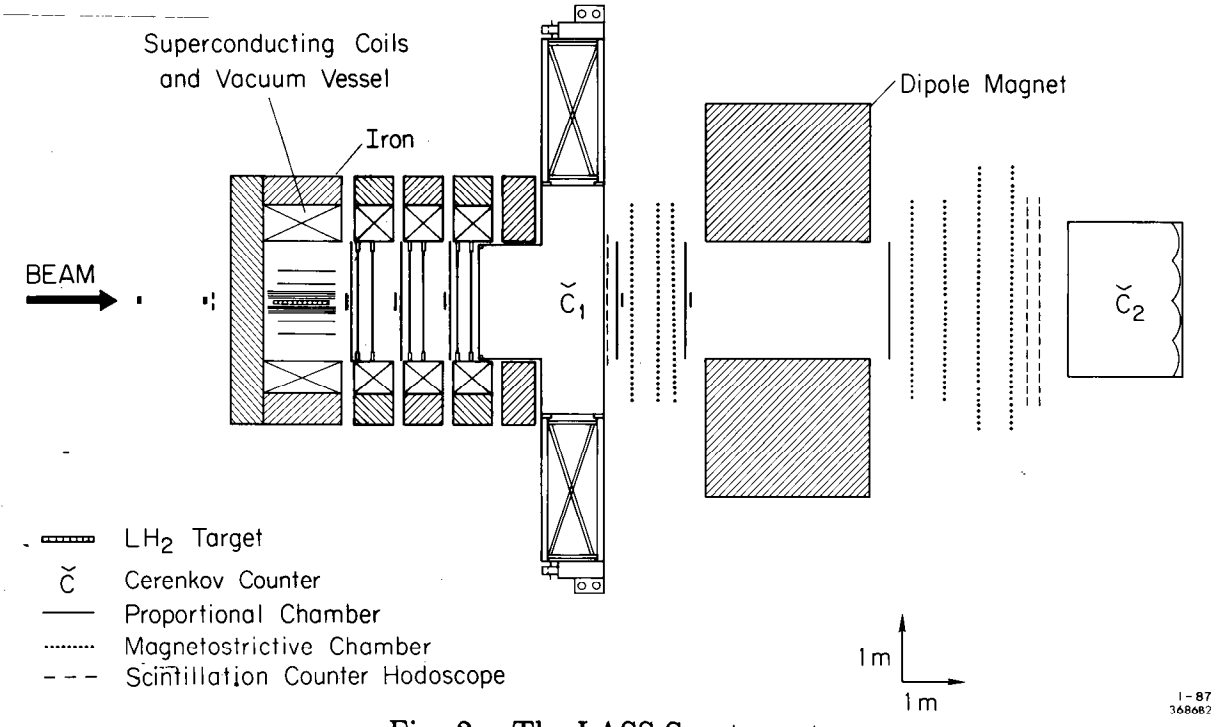

Fig. 2. The LASS Spectrometer.

LASS is situated in an RF-separated beam line which delivers a 5-16 GeV/c beam of high purity (typically 70/1 or better K/π ratio at 11 GeV/c before tagging by beam

Cherenkov counters). The beam is fully analyzed and tagged before entering LASS. The detector is capable of handling a rather high instantaneous flux ($\sim 5 \times 10^6$), but because of the poor duty factor of SLAC (typically 2×10^{-4} at 120 pps), the useful beam flux is limited to ~4/pulse or ~250-500/sec.

The trigger maintains the 4π acceptance by counting particles which emerge from the target in a closed cylinder which surrounds the target. For the K^- program, the trigger is essentially σ_{tot}, except for the all neutral final states, and is quite clean—about 85% of all triggers are good physics events. Under typical conditions, the 6% trigger rate leads to 10–20 events per second to tape. Deadtime starts to be a concern above about 20 events per second. The events average about 3 kbytes each and a 6250 bpi tape is filled about every hour. About 5% of the events are processed during running to check on the data quality. The entire K^- luminosity of 4.1 events/nb (1.13×10^6 events) was taken during running periods totalling about six months spread over a time interval of about two years.

The total LASS (E135) Kaon program contained 135 million events on 2460 raw tapes. Track reconstruction and event classification required about 0.55 seconds per event on an IBM 3081K, so that about 2.4 3081K years were required for one pass through the raw tapes. Since we could only afford to do this job once, some care was given to pre-production testing of small samples before the main analysis was begun. The reconstruction job would be substantially simpler today than it was in 1984/1985 when the processing was actually done. About 36% of the data were processed at SLAC on emulator (168/E, 3081/E) farms which were developed for reconstruction, Monte Carlo, and multi-vertex fitting. The remaining 64% of the data were processed at Nagoya university using the "spare" main frame capacity available on large FACOM computers (an M200 and a M382). The output of the reconstruction process was 1169 DST's (and 225 mini-DST's) classified by topology. For typical processes, reasonable sample sizes could then be attained rather quickly using simple cuts.

The number of people involved in the LASS program has been quite modest by high energy physics standards. The spectrometer itself was designed and operated over about a ten year period which ended with the running of the E135 program in 1982. The Kaon program discussed here (experiment E135) was proposed in 1979. Analysis is still underway. There were 37 physicists in all who worked on the experiment. Twelve of these were students. About nine of these individuals were "core" staff in the sense that they contributed five or more FTE years during the LASS period.

FEATURES OF THE SPECTROMETER PERFORMANCE

Experiment E135 in LASS represents a particular experimental "style" in spectroscopy. It can be thought of as a very large "electronic bubble chamber" exposure with particle identification, rather than a typical selectively-triggered spectrometer experiment. In particular, it emphasizes a broad programmatic approach to the physics which requires (1) a 4π spectrometer with good resolution and particle identification; (2) an open trigger with many different final states (and different production amplitudes); (3) very high statistics; and (4) complete analysis including partial wave decomposition. In this section, a few examples from E135 will be discussed to illustrate some of these features and the relationships between them.

The reaction

$$K^- p \rightarrow K^- \pi^+ n \tag{1}$$

is an ideal place to study the orbital excitation ladder.[3] It is topologically simple, is restricted to the natural spin-parity series, and has a large cross section which is dominated by π exchange at small values of momentum transfer ($t' = t - t_{min}$). The first three orbitally excited leading K^*'s appear as bumps in the raw mass distribution shown in Fig. 3. However, even with the large statistics of this channel the higher mass leading states are hidden, and, of course, none of the interesting underlying structure can be studied in detail without a partial wave analysis (PWA). Thus, sufficient resolution to select the channel, and very good acceptance in the $K\pi$ angular variables are basic requirements. Note that the "effective" statistics which are available are reduced by the need for data selection cuts, as illustrated in Fig. 3.

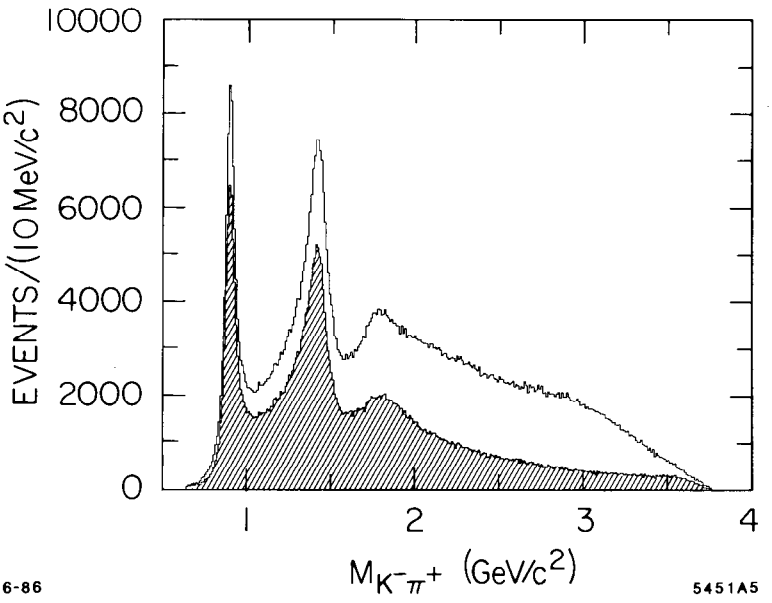

Fig. 3. The invariant $K^-\pi^+$ mass from the reaction $K^- p \rightarrow K^-\pi^+ n$ for $|t'| \leq 1.0$ $(GeV/c)^2$; the unshaded curve contains all 730,000 events while the cross-hatched curve contains the 385,000 events that remain after the N^* is removed.

For example, removing the nucleon resonance region costs about a factor of two in statistics, and after selecting the events which are useful for a study of $K\pi$ scattering ($t' \leq 0.2$ $(GeV/c)^2$) the data sample available for analysis is about 151,000 events. The number of K^* states is large, and the states interfere and overlap so that this statistical level turns out to be just adequate to sort out the full structure in the

mass region up to about 1.85 GeV/c^2, while at higher masses only the leading states can be seen with confidence. Figure 4 shows the observed P-wave structure in the region below 1.8 GeV/c^2. In addition to the well known $K^*(890)$, there is a state (the $K^*(1790)$) sitting underneath the leading $K_3^*(1780)$, and a state with very small elasticity (6.6%) around 1.4 GeV/c^2. The observation of such a small branching ratio clearly requires the full statistical power of the experiment, and even so, confirmation is needed before such a state can be accepted as fully reliable.

Historically, in LASS these observations of the two underlying 1^- states in the 1.4 to 1.8 GeV/c^2 region confirmed results from the reaction

$$K^-p \to \overline{K}^0\pi^+\pi^-n. \qquad (2)$$

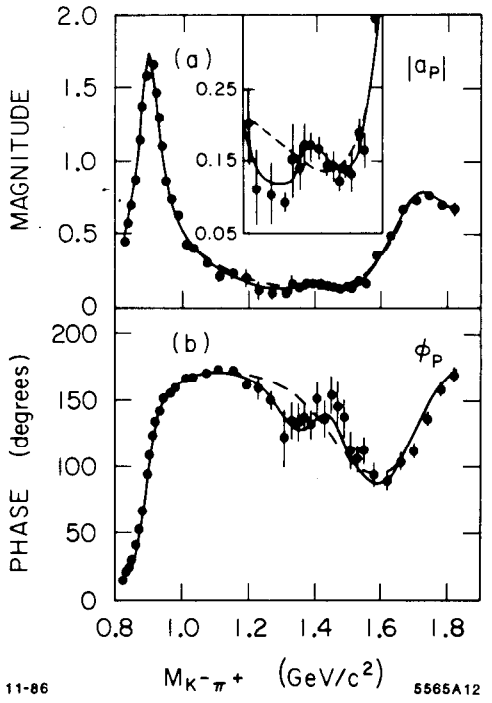

Fig. 4. The magnitude (a) and phase (b) of the $K^-\pi^+$ P-wave amplitude from the reaction $K^-p \to K^-\pi^+n$ in the mass region below 1.84 GeV/c^2. The dashed line shows the results of a fit including the $K^*(892)$ and $K^*(1790)$ only, while the solid line indicates the fit that includes another resonance around 1.4 GeV/c^2.

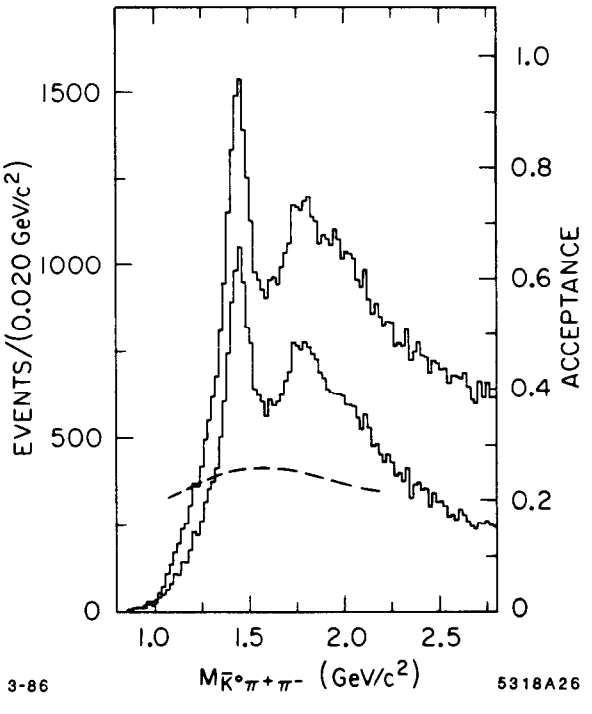

Fig. 5. The invariant $\overline{K}^0\pi^+\pi^-$ mass from the reaction $K^-p \to \overline{K}^0\pi^+\pi^-n$ for all events (top) and for events with $|t'| \leq 0.3$ (GeV/c)^2 (bottom); the dashed line gives the final acceptance after all cuts.

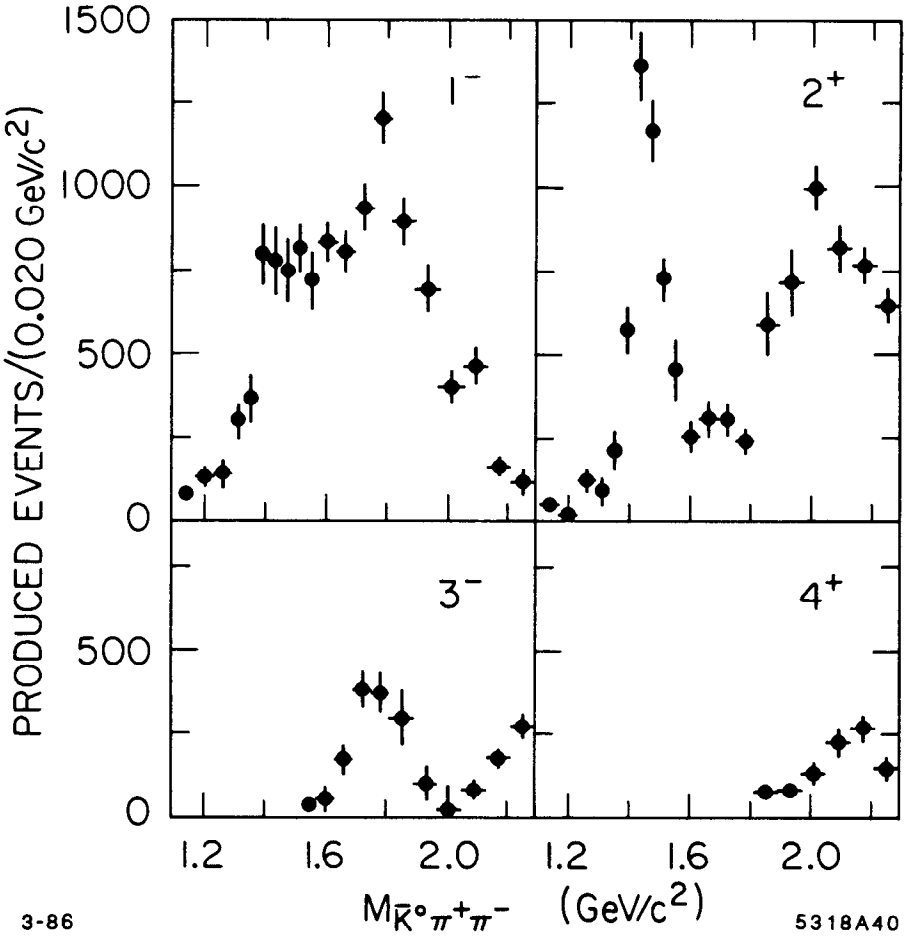

Fig. 6. The natural spin-parity wave sums from the reaction $K^-p \to \overline{K}^0\pi^+\pi^-n$.

The invariant mass distribution shown in Fig. 5 for reaction (2)[5] is reminiscent of that shown above for reaction (1). It looks quite simple with bumps around the leading $K_2^*(1430)$ and $K_3^*(1780)$ resonances above a rather smooth "background." In fact, the PWA demonstrates that over two-thirds of the spectrum is resonant, and that the peaks around 1.45 and 1.8 GeV/c^2 each contain important contributions from at least two resonances. For example, the natural spin-parity J^P sums (Fig. 6) show the leading $2^+, 3^-$, and 4^+ natural spin-parity resonances as bumps in the J^P cross sections, but bumps in the 1^- cross section are about as large around 1.4 and 1.75 GeV/c^2 as the leading resonances. A further decomposition of the 1^- amplitude into the different isobar partial waves (Fig. 7) shows that the structures are caused by two 1^- states which are consistent in parameter values with those seen in reaction (1). The lower state has a mass of 1.42 ± 0.017 GeV/c^2 and couples mostly to $K^*\pi$ while the higher state has a mass of 1.735 ± 0.030 GeV/c^2 and couples to both $K^*\pi$ and $K\rho$. The production characteristics of these states are also consistent with the observed $K\pi$ elasticities. The simplest classification of these objects is that the lower

mass state is the 2^3S_1 K^* and the higher mass state is 1^3D_1. From an experimental perspective, the observation and confirmation of these states benefited greatly from essentially all of the stylistic features of the experiment noted above.

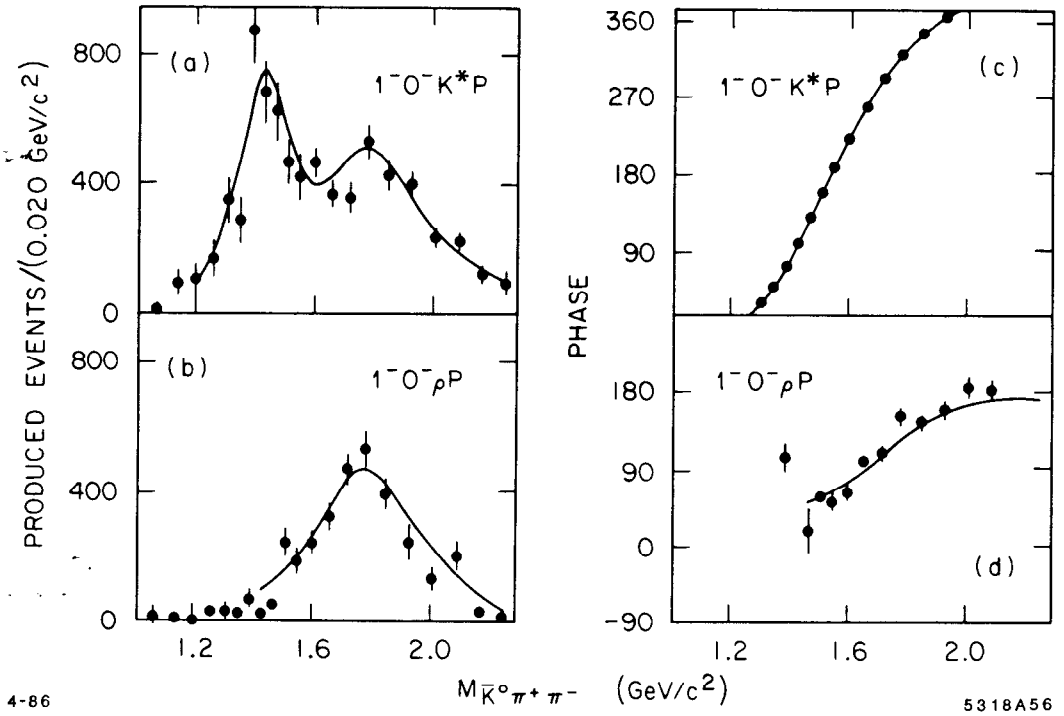

Fig. 7. The $1^-\overline{K}^0\pi^+\pi^-$ P-wave amplitudes from the reaction $K^-p \to \overline{K}^0\pi^+\pi^-n$ showing a $K^*(1410)$ coupling mostly to $K^*\pi$ and a $K^*(1790)$ coupling to both $K^*\pi$ and $K\rho$.

The high sensitivity and excellent acceptance of LASS are also important to the study of much lower cross section channels such as

$$K^-p \to K^-K^+\Lambda, \tag{3}$$

and

$$K^-p \to K^0_S K^0_S \Lambda. \tag{4}$$

These reactions[8-10] are restricted to natural spin-parity mesons only, and are dominated by peripheral hypercharge exchange. The production of $s\bar{s}$ mesons is therefore expected to be greatly favored over glueballs. These channels should provide a clear look at the strangeonia, and also lead to revealing comparisons with the same final states seen in other production channels which might be glue-enriched. The selection of reaction (3) is particularly sensitive to good particle identification and both channels depend on the ability to reconstruct the slow Λ. The study of the meson systems makes essentially the same experimental demands on the spectrometer as discussed above for the study of reactions (1) and (2).

The mass spectrum [Fig. 8(a)] for reaction (3) shows bumps corresponding to the well-known $\phi(1020)$ and $f_2'(1525)$ leading orbital states, as well as a smaller bump in the $\phi_3(1850)$ region. Only the $f_2'(1525)$ is clearly seen in reaction (4) [Fig. 8(b)] since this channel is restricted to the even spin states. In neither case is there any evidence for the $\theta(1720)$. In general, the K^-K^+ (strangeonium) spectrum is very reminiscent of the $K^-\pi^+$ (strange) spectrum (Fig. 3) with an appropriate shift in mass scale to account for the additional constituent s quark. This should be contrasted with production of the same final state with a π beam, as observed in the CERN Ω spectrometer,[20] where no strangeness is exchanged. Figure 9 compares the mass spectrum observed in the π beam case with the results from reaction (3). The bumps observed are associated with minority decay modes of objects without hidden strangeness, such as $f_2(1270)$ and $a_2(1320)$, interfering with strangeonium production.

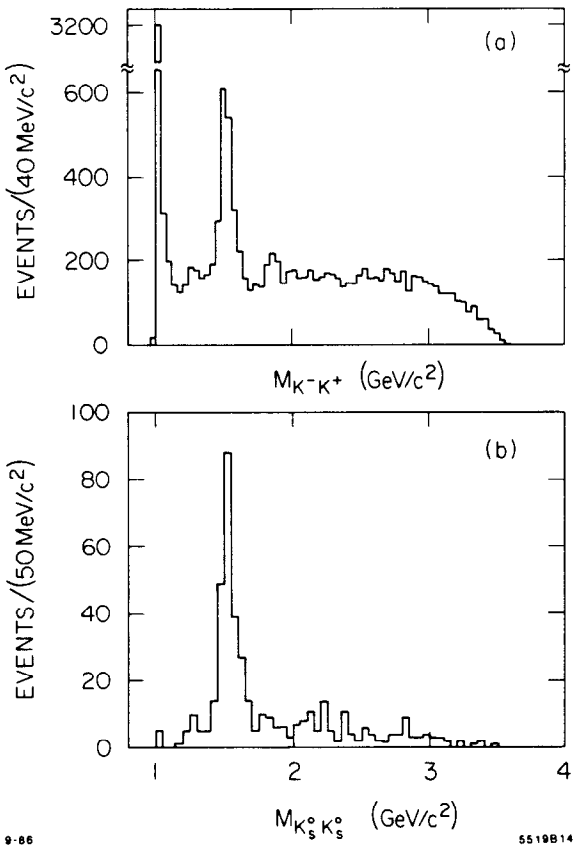

Fig. 8. The $K\overline{K}$ mass spectra from reaction; (a) $K^-p \to K^-K^+\Lambda$; and (b) $K^-p \to \overline{K}^0K^0\Lambda$.

Even though the sample sizes are much smaller for the strangeonium channels than for the strange ones, the spectroscopy is expected to be very similar; and, in principle, a full spin analysis is necessary to understand the details of the spectrum. In E135, the statistics are not available to allow this in detail, and little can be done to probe the underlying states above 1.6 GeV/c^2. However, since the acceptance of the spectrometer is very good, the nature of the leading strangeonia up to G-wave can be studied in reaction (3) in the following way. It is first shown that the interference between $s\bar{s}$ resonance production and diffractive N^* production can be utilized to analyze the leading $s\bar{s}$ amplitude, and this method gives results which are consistent with a more conventional spin-parity analysis in the F-wave region where the statistics are sufficient to perform the more conventional analysis. The method is then extended to the analysis of the G-wave amplitude in the 2.2 GeV/c^2 region. Figure 10 shows evidence for a 4^{++} state ,the $f_4'(2210)$, which is a good candidate to be the mainly $s\bar{s}$ member of the 4^{++} nonet predicted by the quark model.

It is appropriate here to look a bit more directly at the issues of spectrometer acceptance and its effect on the physics analysis. Figure 11 compares the raw invariant $K^-\pi^+$ mass spectra from reaction (1) as seen in three different experiments done at SLAC.[3,21,22] All of these experiments were designed to do high quality studies of

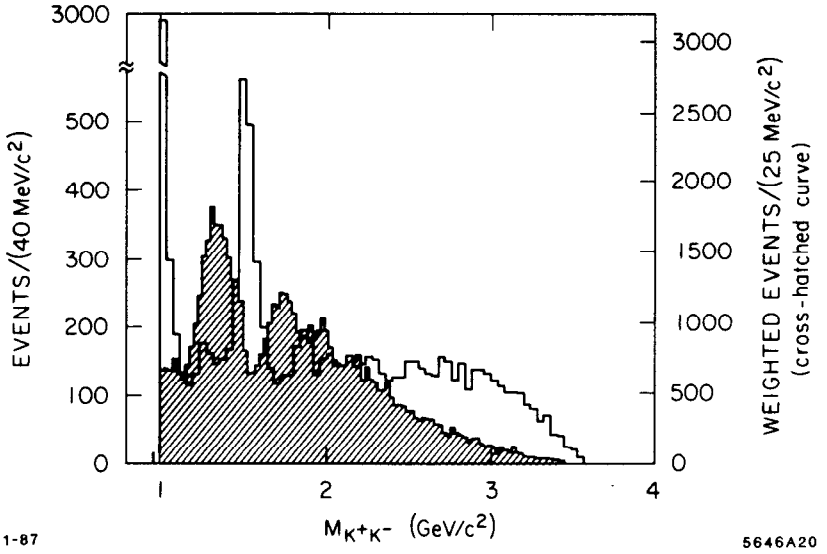

Fig. 9. Comparison of the K^-K^+ mass spectra from the reaction $K^-p \to K^-K^+\Lambda$ seen by the LASS experiment (unshaded) with that from the reaction $\pi^-p \to K^-K^+n$ (cross-hatched) seen in the Ω spectrometer at CERN.

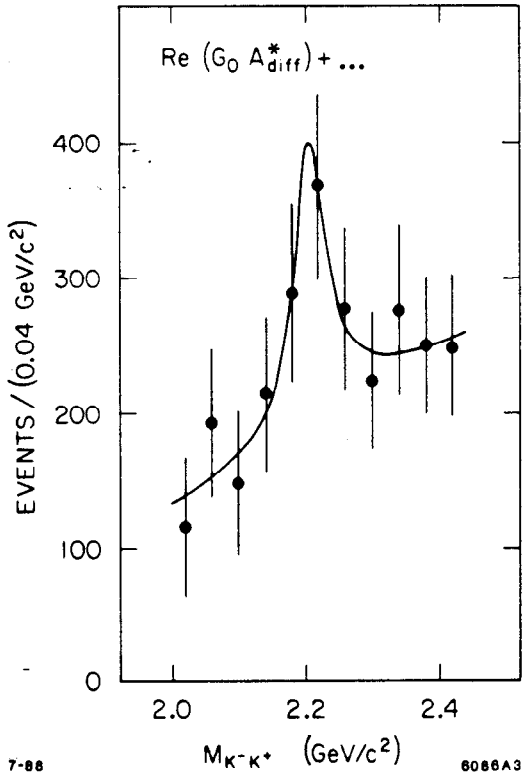

Fig. 10. The mass dependence of the interference between the K^-K^+ G_0 and diffractive background amplitudes from the reaction $K^-p \to K^-K^+\Lambda$ showing evidence for a 4^{++} state around 2.2 GeV/c^2.

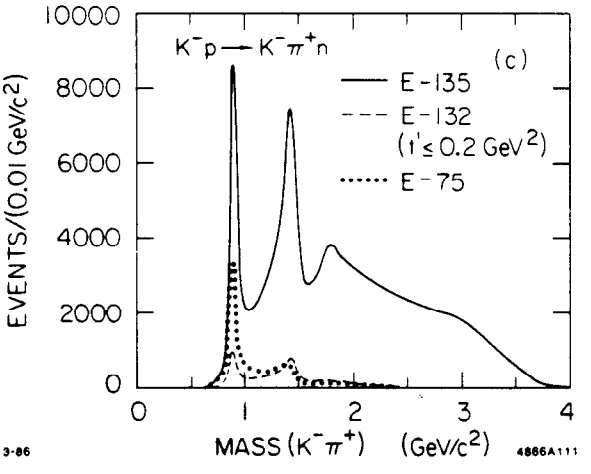

Fig. 11. Comparison of the invariant $K^-\pi^+$ mass spectra from the reaction $K^-p \to K^-\pi^+n$ as seen in three different spectrometers.

reaction (1) and had somewhat comparable amounts of running time—E132 had the shortest running period. The solid line is from E135 and has very little distortion since the spectrometer and trigger are essentially full-acceptance. The dashed line is from an earlier experiment in LASS (E132) which also had nearly 4π reconstruction acceptance but had a two-particle forward trigger which reduced the effective acceptance for states at high mass with high spin. The experimental sensitivity is less, of course, which reduces the event sample, but the trigger bias distorts the high mass behavior as well. The dotted line is taken from the forward-dipole spectrometer experiment E75. A significant amount of distortion of the spectrum already occurs by a mass of 1.4 GeV/c^2. This distortion occurs because the data from high spin objects preferentially populate the ends of the angular distribution. The loss of these data can clearly be seen by comparing the scatter plots of mass versus the cosine of the helicity angle in the Gottfried-Jackson frame ($cos\theta_J$) for E75 (Fig. 12) and ($cos\theta_{GJ}$) for E135 (Fig. 13).

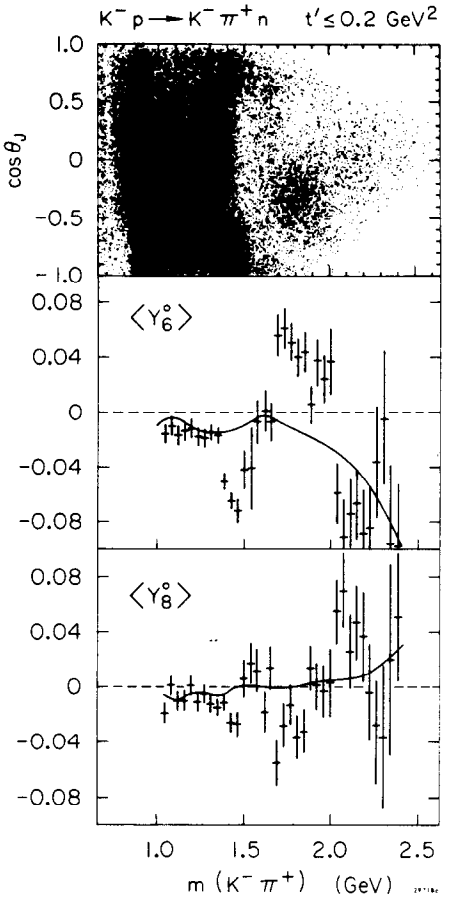

Fig. 12. Scatter plot of the $K^-\pi^+$ mass against $\cos(\theta_J)$ from the reaction $K^-p \to K^-\pi^+n$ in the region $|t'| \leq 0.2\ (GeV/c)^2$ as seen in the dipole spectrometer of experiment E75. The L=6,8 M=0, uncorrected spherical-harmonic moments Y_L^M as functions of mass are also shown; the solid line shows the effect of the spectrometer acceptance.

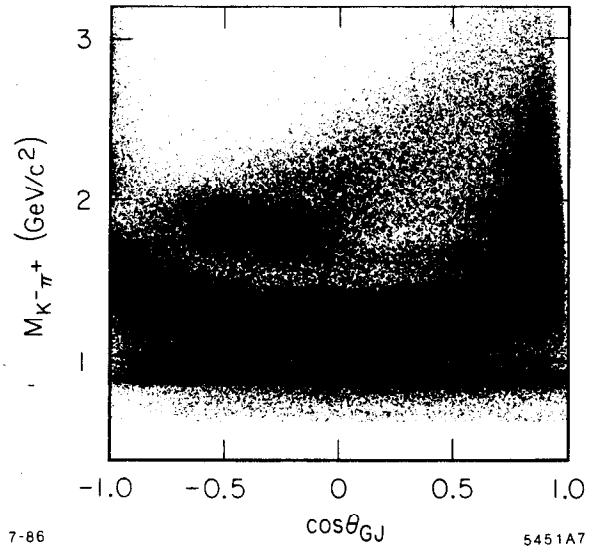

Fig. 13. Scatter plot of the $K^-\pi^+$ mass against $\cos(\theta_{GJ})$ from the reaction $K^-p \to K^-\pi^+n$ in the region $|t'| \leq 0.2\ (GeV/c)^2$ as seen by E135 in LASS.

Good resolution is also crucial, both for sample selection and for the observation of narrow structures; and it should be good over the entire phase space. For example, the two body mass resolution needs to be sufficient to resolve narrow structures such as the $\rho - \omega$ interference effect shown in Fig. 14 for the reaction[15]

$$K^- p \rightarrow \pi^- \pi^+ \Lambda. \tag{5}$$

Good resolution in missing mass is also important in the selection of channels with a neutral recoil. Figure 15 shows the squared missing mass distribution (MM^2) against the $K^-\pi^+$ system from reaction (1). There are significant backgrounds which can arise both above and below the neutron recoil, and the resolution should be sufficient to separate these backgrounds from the desired neutron recoil. The background remaining in the neutron sample after cuts is estimated from the fit to the distribution of Fig. 15 to be 6%.

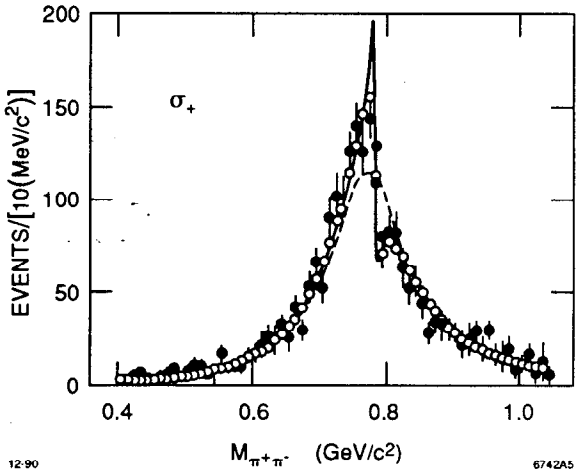

Fig. 14. The natural parity exchange cross section in the ρ region from the reaction $K^- p \rightarrow \pi^- \pi^+ \Lambda$. The data are shown as solid dots; the solid curve represents a fit expression which includes $\rho - \omega$ interference; the open dots represent the resolution smeared curve; and the dotted curve is the contribution from the ρ line-shape only.

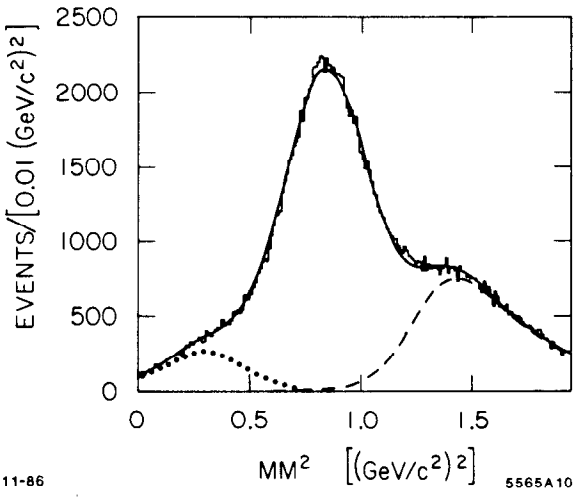

Fig. 15. The squared missing mass distribution against the $K\pi$ system from the reaction $K^- p \rightarrow K^- \pi^+ n$ for events with $|t'| \leq 0.2\ (GeV/c)^2$. The solid line indicates the results of a fit which includes the experimental resolution and background contributions from the $K^-\pi^+\Delta^0$ (dashed line) and $K^-\pi^0 p$ (dotted line) final states.

Good resolution coupled with good acceptance can also be thought of as a form of "particle identification" and allows otherwise inaccessible channels to be studied. For example, the reaction

$$K^- p \rightarrow K^- \eta p \tag{6}$$

was studied in E135 in a missing π^0 mode.[6] Figure 16(a) shows the raw $K\eta$ invariant mass dependence, while the intensity distributions for the D and F waves are shown in Figs. 16(b) and 16(c). There is a significant amount of $K_3^*(1780)$ seen but no $K_2^*(1430)$.

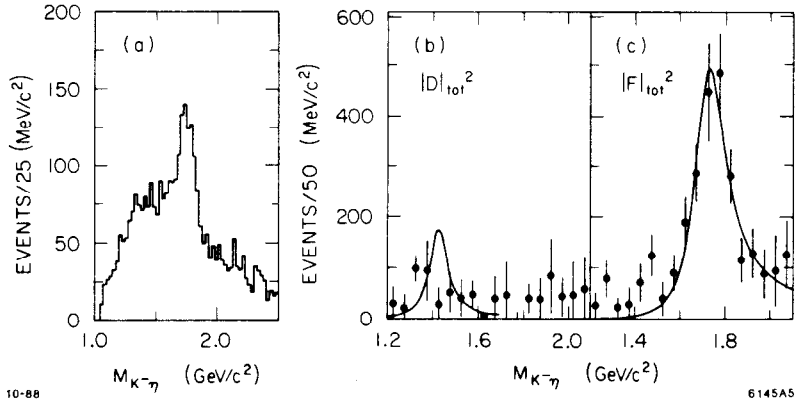

Fig. 16. The $K\eta$ mass dependence from the reaction $K^-p \to K^-\eta p$ for: (a) the raw data spectrum with $M(\eta p) \geq 2.0$ GeV/c^2 and $M(K^-p) \geq 1.85$ GeV/c^2; (b) the intensities of the D and (c) F waves; the Breit-Wigner curve on the D wave indicates the 95% upper limit for $K_2^*(1430)$ production while the curve on the F wave indicates the fit to the $K_3^*(1780)$.

Finally, direct particle identification is important, and is used throughout the sample selection of most of the channels described above. As one further example of the power of this technique for spectroscopy, it is instructive to consider the $\Xi^0(1530)K^-$ mass distribution shown in Fig. 17.[4]

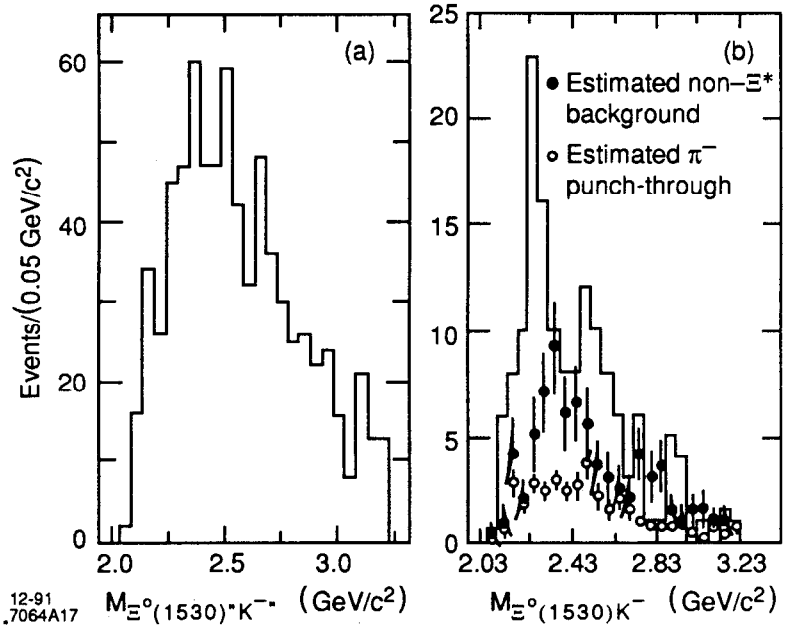

Fig. 17. The $\Xi^0(1530)K^-$ mass distribution for: (a) all events where the "K^-" is actually identified by the particle identification system as a π; (b) for events where the "K^-" is identified as a true K^-.

When the particle called a K^- is actually identified by Cherenkov or TOF as a π, Fig. 17(a), there is a smooth mass distribution. However, when the particle is positively identified as K^- the distribution, shown in Fig. 17(b), has a sharp structure around 2.25 GeV/c^2 which provides clear evidence for production of the $\Omega^{*-}(2253)$.

In summary, the LASS experience has demonstrated the power of the programmatic "electronic bubble chamber" approach to experimental meson spectroscopy. The experimental difficulties inherent in performing these experiments were tractable. In particular, the beam requirements were modest; the computing needs were met in a straightforward manner; the analysis tools were developed to perform the required studies of even the highest statistics channels; and the number of physicists required by the experiment was modest. In the following sections, I would like to explore how this experience might be extrapolated to possible future facilities and experiments.

A FUTURE SPECTROSCOPY FACILITY

In the following section, I will review a few desirable features of a new facility for meson spectroscopy and some of the experiments which might be performed there. I caution the reader that this is a highly selected, personally biased, and somewhat idiosyncratic list.

The Experimental Program

Ideally, it seems clear that two complementary approaches to high "luminosity" experiments should be pursued in the future. The first approach utilizes a clever trigger which can be used with a high flux beam into a good spectrometer to select low cross section processes and study them with high statistics. Though this approach has many attractions, and in the case of low cross section channels may represent the only possible way to do the experiments, the number of topics which can benefit from this approach is limited by the difficulty of devising efficient triggers which maintain 4π acceptance. Moreover, it is not a very efficient way to use beam time since most of the physics is not written to tape. The second approach is to extend the LASS style experiment discussed above by a factor of $\sim$ 100 or more, using all possible incident beams (π, K, p) to allow the various spectroscopies to be compared and contrasted. The advances that could be expected from such a program are enormous. For example, for a K^- beam, the number of events expected in a few of the final states which might be useful for the study of the strange mesons are given in Table 1.

The attainment of this level of statistics would be expected to lead to an excellent understanding of the strange meson spectrum at least up to the $K_5^*(2380)$, with good measurements of the masses and widths, branching ratios, multiplet splittings, etc. At the same time, the events available in channels for studying strangeonia would become comparable to the statistics now available in E135 for the strange meson studies, as shown for a few examples by Table 2 below, and should lead to a rather complete understanding of the strangeonia, including underlying states, below about 2.0 GeV/c^2.

Table 1

Strange Channels	
Final State	**Expected Number of Events**
$K^-\eta p$	7 x 10^5
$\overline{K}^0\pi^- p$	2 x 10^6 above the $K_2^*(1430)$
$K^-\pi^+ n$	4 x 10^7 above the $K_2^*(1430)$
$K^-\omega p$	1 x 10^7
$K^-\phi p$	2 x 10^6

Table 2

Strangeonium Channels	
Final State	**Expected Number of Events**
$K^-K^+\Lambda$	1 x 10^6
$\overline{K}^0K^0\Lambda$	5 x 10^4
$\overline{K}^0K^\pm\pi^\mp\Lambda$	4 x 10^5
$\overline{K^*}K^*\Lambda$	1 x 10^5

The Spectrometer

In the following, I would like to consider some of the design features of a facility to perform the broad programmatic spectroscopy program discussed in the preceding section. In general, the LASS spectrometer appears to be an excellent model for a new facility. Of course, it should be improved in a number of major ways, and in any case it no longer exists, so that an all new device is a necessity. Some of the improvements which might be incorporated are:

1. Modern technology tracking detectors to improve overall tracking efficiency and resolution, and to improve the vertex finding and resolution. The chambers should also incorporate high quality dE/dx measurements to improve the particle identification in the $1/\beta^2$ region.
2. Better geometrical matching between the solenoid and the dipole magnets (LASS used a rather small "recycled" dipole).
3. A shorter LH_2 target to improve the geometry in the vertex region. However, the optimization of the target length also depends on the beam flux available and the trigger rate of the detector.

4. Modernization of the particle identification. In principle, ring imaging Cherenkov detectors could cover essentially all of the phase space of the experiments, but their cost would need to be justified.
5. Added shower detectors. However, a 4π photon detection system would be expensive and would also require a larger solenoid.
6. Improvement of the trigger and the data acquisition systems to handle very high rates.

The Beam

There are a number of constraints on the choice of the optimum beam momentum for spectroscopy experiments. From a physics perspective, access is needed to meson masses of at least 2.5 GeV/c^2, which implies that the beam momentum should be greater than about 8 GeV/c. The overlap of the meson resonance region of interest with the low mass baryon resonance recoils should also be minimized, which pushes the desired momentum up. On the other hand, exclusive cross sections drop as the momentum goes up. From an experimental perspective, as beam momenta increase, the experiments tend to grow physically larger, since the resolution in the final state variables must be maintained. Particle identification technologies also tend to fill specific energy niches, and, in particular, high momentum particle identification is quite difficult. Taking all these factors into account, there seems to be a rather broad optimum momentum range for light quark spectroscopy around 10–20 GeV/c, but higher energies can certainly be accommodated with an appropriate spectrometer design.

The flux and cleanliness requirements on this beam appear to be quite modest. In an experiment with a restrictive trigger, the beam flux will be limited by the rate tolerance of the detector, and the cleanliness of the beam is the limiting factor; but for a more open trigger, the limiting factor is more likely to be the acquisition rate of the spectrometer. If the experiment runs in a mode which saturates the event acquisition capability at 1000 Hz, then with a 10 cm LH_2 target and a 10 GeV/c K^- beam, the average flux of useful particles required is $\sim$ 2 x 10^5/sec. The maximum flux into a 4π spectrometer is limited by the tolerance of the detectors to tracks from events and background. Since there is a substantial amount of material in the beam, it is unlikely that a detector with conventional gaseous tracking detectors will be able to tolerate an instantaneous flux much greater than $\sim$ 1 x 10^7. Thus, the ratio of the desired particle to total flux must be around 1/50 or better. Depending on the machine energy, particle type, duty factor, and trigger rate, an RF-separated beam may (or may not) be required for minority particle (e.g. Kaon) beams.

CPU Power and Data Storage

The cost/performance ratio of computing equipment has been improving rapidly since the LASS experiment, and it now appears unlikely to be a crucial issue for the experimental program being considered here. None the less, the requirements are significant and need to be addressed as a part of the facility design. If we assume that the requirements are arbitrarily defined to be 100 times LASS per calendar year, the new experiment would need to transfer 6 Mbytes/sec of data leading to a total data storage need of 50 terabytes per year. The basic CPU processing requirement for

reconstruction would be about 5000 MIP's. There appears to be no difficulty meeting the latter requirement. The current best price/performance leader (a HP 9000/720) costs $\sim$ \$210/MIP. Thus, a 5000 MIP facility would cost about \$1M at present prices. It will surely be less next year.

Meeting data storage and channel rates requirements appears to be more problematic.[23] Present technologies are marginal. For example, 8 mm tapes have rather high capacity (2500 Mbytes/tape), and the drives and tapes are inexpensive, but the transfer rate is between 1 and 2 orders of magnitude too slow. Standard 3480 silos have adequate transfer capabilities, but the cartridges have low capacity ($\sim$ 200 Mbytes per cartridge or 5×10^5 tapes/year), and silo slots cost about \$50 each. There are some future technologies on the horizon which would probably match the requirements. For example, Sony has developed a digital instrument recorder using 19 mm tape which can store 0.1 terabytes/tape. The units are projected to cost about \$250k each and have a transfer rate of $\sim 1 - 30$ Mbytes/sec. Digital paper tape technologies are also tantalizing. They would be expected to reach transfer rates of $\sim$ 3 Mbytes/sec, and to store 1 terabyte/tape. The drives are modest in cost ($\sim$ \$200k per drive) but the paper tapes are expensive ($\sim$ \$10k per tape). Since the number of tapes used per year is very small, however, it might be viable.

Since CPU horsepower is so cheap, and since physics (four-vector) DST's could easily be an order of magnitude more compressed than raw data, it is tempting to consider doing data reconstruction at the time the data are acquired and discard the raw data entirely. The data would then be ready for analysis as it was taken and the data storage problem would be significantly reduced. This implies that the spectrometer must be fully aligned and the software tuned before the bulk of the data are taken. Though this is not impossible in principle, it seems quite difficult to manage in practice. In LASS, for example, much of the raw data was carried along onto the DST's for use in the final analysis stages. One could also try to devise a trigger or filter which puts only a desired subsample of events to tape. However, it is difficult to maintain a full 4π spectrometer unless the trigger is very sophisticated, and then the software and spectrometer must be well understood as the data are acquired. Thus, it would appear that some provision for full data storage of at least a portion of the experiment will be required in any case.

CONCLUDING REMARKS

A new fixed target facility for meson spectroscopy could make a significant, lasting impact on our understanding of light quark mesons and exotica. However, such an experiment is a substantial effort. It requires (1) a very high quality spectrometer with 4π acceptance, full vertex reconstruction, particle identification, γ detection, and a high ($\sim$ 1kHz) data-taking rate; (2) very large data samples ($\sim 10^{10}$ events); (3) lots of data storage and CPU horsepower; (4) sophisticated analysis programs; and (5) long term commitment from a laboratory and a group of experimentalists and interested theorists to the complete program. The beam flux requirements for most of the program are not particularly severe, and could probably be attained at a number of existing accelerators as well as at the new "factory" machines. However, at the moment, it appears that the required institutional commitment to the program is unlikely to be available at existing facilities, so that the performance of this experiment may "de-facto" await the construction of a high flux "factory."

ACKNOWLEDGEMENTS

I would like to thank the members of the LASS group, whose work has provided most of the material for this talk.

REFERENCES

1. See, for example, contributions to this conference by D. Lazarus, and Yu. D. Prokoshkin.
2. D. Aston et al., The LASS Spectrometer, SLAC Report 298 (1986).
3. D. Aston et al., Phys. Lett. 180B (1986) 308; Nucl. Phys. B296 (1988) 493.
4. D. Aston et al., Phys. Lett. 194B (1987) 579.
5. D. Aston et al., Nucl. Phys. B292 (1987) 693.
6. D. Aston et al., Phys. Lett. 201B (1988) 169.
7. D. Aston et al., Phys. Lett. 201B (1988) 573.
8. D. Aston et al., Nucl. Phys. B301 (1988) 525.
9. D. Aston et al., Phys. Lett. 208B (1988) 324.
10. D. Aston et al., Phys. Lett. 215B (1988) 199.
11. D. Aston et al., Phys. Lett. 215B (1988) 799.
12. P. F. Bird Ph.D. Thesis, SLAC Report 332 (1988).
13. D. Aston et al., SLAC-PUB-5150 (1989).
14. D. Aston et al., SLAC-PUB-5634 (1991).
15. D. Aston et al., SLAC-PUB-5657 (1991).
16. D. Aston et al., Invited Talks at this Conference; SLAC-PUB-5721 and SLAC-PUB-5722 (1991).
17. B. Ratcliff et al., Invited Talk at this Conference, and SLAC-PUB-5682 (1991).
18. See, for example, S. Godfrey and N. Isgur, Phys. Rev. D32 (1985) 189.
19. See, for example, PDG, Phys. Lett. 239B (1990) and references therein.
20. C. Evangelista et al., Nucl. Phys. B154 (1979) 381.
21. P. Estabrooks et al., Nucl. Phys. B133 (1978) 490.
22. D. Aston et al., Phys. Lett. 106B (1981) 235.
23. J. Pfister, in AIP Conference Proceedings 209 (1990) 503.